New Journal of Physics
The open-access journal for physics

Universal nanocolloid deposition patterns: can you see the harmonics of a Taylor cone?

Xinguang Cheng and Hsueh-Chia Chang[1]
Department of Chemical and Biomolecular Engineering, University of Notre Dame, Notre Dame, IN 46556, USA
E-mail: hchang@nd.edu

New Journal of Physics **11** (2009) 075023 (9pp)
Received 27 January 2009
Published 31 July 2009
Online at http://www.njp.org/
doi:10.1088/1367-2630/11/7/075023

Abstract. Specific harmonics of the Laplace equation are selected near a conducting Taylor cone with discrete polar angles for the field maxima. Charged nanocolloids ejected along the discrete electric field lines of these mode maxima are observed to deposit a universal spectrum of rings on an intersecting plane, with particles of different sizes occupying different spectral lines due to different residue charge. After an affine transformation, nanocolloids ejected into a microslit and deposited onto one substrate are also shown to exhibit the same universal line spectra.

Contents

1. Introduction and the harmonics of Taylor cone

Electrospray is widely used to produce nanosized drops for protein and DNA characterization [1], microencapsulation [2] and nanocolloid synthesis [3]. Micron-sized drops are ejected from the Taylor cone [4] and reach nanometer size due to evaporation and Rayleigh fission [5].

[1] Author to whom any correspondence should be addressed.

There is also increasing effort to analyze the electrophoretic mobility of charged bioparticles like bacteria and other solid bioaerosols by electrospray in a class of colloid spectrometry sometimes known as differential mobility analysis [6]. With their larger inertia compared to molecules, colloid charging and ejection from a Taylor cone are insensitive to thermal noise and colloid spectrometry can often be done at atmospheric conditions. Moreover, the deterministic nature of the electrophoretic colloid trajectories can exhibit intriguing patterns that can allow better spectroscopic characterization. In this paper, we report the selection of multiple discrete trajectories by nanocolloids ejected from a Taylor cone, resulting in discrete deposit lines with universal spectral features. Competitive selection of these spectral lines by colloids of different sizes is also established to further advance the possibility of exploiting the universal spectral lines for characterization purposes.

The discrete spectra of the Laplace and Schrodinger equations are responsible for discrete frequencies and energy levels in vibration and quantum mechanics, manifested through specific time-periodic standing wave harmonics. For example, we have employed ac electric fields of specific frequency to excite certain Rayleigh–Lamb harmonics of a meniscus to achieve rapid nanodrop ejection [7]. The dc Taylor cone free-surface electrostatics selects certain discrete harmonics (the static variety) by an entirely different mechanism. Because of radial symmetry about the cone axis, only axisymmetric spherical harmonics of the Laplace equation are activated near an equipotential cone defined by the usual Legendre polynomial in spherical coordinates, $\phi_n = r^n P_n(\cos\theta)$. The normal Maxwell stress $\varepsilon|\nabla\phi|^2/2$ at the conducting cone interface must balance the singular normal capillary stress $\gamma\nabla\cdot\mathbf{n}$ even when the latter becomes singular at the tip with a scaling of $1/r$ with respect to the cone radius r. As such, a specific cone half-angle of 49.3° (or $\theta_0 = 130.7°$) is obtained [4] with the spherical harmonic $n = 0.5$, which provides the necessary singular Maxwell stress.

However, a discrete number of axisymmetric spherical harmonics, $r^n P_n(\cos\theta_0) = 0$, parameterized by the non-integer mode number n, can actually be selected by the conducting Taylor cone with the above half-angle for $n = 0.5,\ 1.892\,34,\ 3.275\,19,\ 4.655\,25,\ 6.034\,13,\ 7.412\,42,\ 8.790\,37,\ 10.1681, \ldots$, which will be enumerated as modes $m = 0, 1, 2, 3, \ldots$. Near the cone, the field intensity of each successive mode decays as r^{n-1} and only the first mode is singular. The zeroth mode with $n = 0.5$ is the one that ensures normal stress balance but the others can also be excited. As the field strength decreases with mode number, we shall consider only these dominant modes. Only modes 2 and higher exhibit discrete field maxima with polar angles θ between 0° and 90°, the angle window for the spray, as shown in figure 1, yielding a total of six relevant modes. Modes 3 and higher can exhibit multiple distinct off-axis field extrema at specific nonzero angles, as shown in figure 1 for two of the modes, as well as a dominant maximum at zero polar angle. Two dominant field maxima exist within polar angles between 90° and 45°, belonging to the dominant modes $m = 2$ and 3. These two maxima are located at polar angles 78.4° and 58.7°. However, a bunch of field maxima with similar values appear when the polar angle decreases below 42.8°, where a field maximum of mode 3 appears. As all modes share a field maximum along the cone axis, we shall scrutinize an angle window away from the axis. A total of nine discrete maxima are found with polar angles θ between 20° and 55° for the six dominant modes. (These will be shown to be the relevant field maxima for a subsequent experiment that uses a slot to capture particles ejected within this angle range.) Only five of the dominant 6 modes have field maxima that can be represented in this polar angle range, corresponding to $n = 4.655\,25, 6.034\,13, 7.412\,42, 8.790\,37, 10.1681$ ($m = 3$, 4, 5, 6 and 7). Among the nine lines, mode 7 appears three times and modes 5 and 6 appear

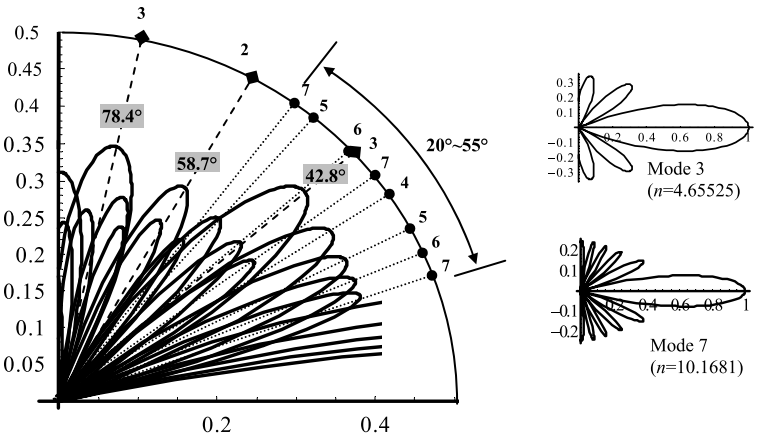

Figure 1. Equipotential lines of the axisymmetric harmonics of a conducting Taylor cone in spherical coordinates whose origin lies at the cone tip. Two specific harmonics (3rd and 7th) are shown as insets with their corresponding n numbers. Rays along the field maxima of the different harmonics produce nine universal ring intersections with a sphere, whose relative separations are independent of the sphere size.

twice with polar angles 20.6°, 23.7°, 27.8°, 33.7°, 37.7°, 42.8°, 43.3°, 50.9° and 54.7° for all nine field maxima. The intersection of these field maxima with a spherical surface produces a universal ring spectrum, whose arc length separation on the spherical cap can be normalized to the first separation between mode 7 with a polar angle of 20.6° and mode 6 at 23.7°. Thus normalized, the eight separations between successive members of the nine rings are 1, 1.35, 1.92, 1.31, 1.66, 0.18, 2.47 and 1.24. These are universal metrics that we shall try to extract from deposited nanocolloid lines.

It should be noted, however, that the field maxima of these discrete harmonics will only appear in the field if a small number of them are present. Far from the cone, where electrodes and other foreign objects excite higher harmonics, the discrete field maxima should be smoothed out. However, near the cone, when only the first few modes dominate, multiple field maxima should exist.

As the spectral modes represented in the universal spectrum of figure 1 have distinct field maxima away from the axis, a ring of counter-electrodes or two electrodes symmetric about the cone axis should favor these modes over the zeroth mode, which does not exhibit field maxima away from the axis. This selection of the multiple discrete harmonics is best realized with charged nanocolloids, whose density is sufficiently low such that space charge effects are not relevant [8] and the Laplace equation remains valid. The relatively large inertia of nanocolloids, as compared to nanodrops or ions, also eliminates smearing of the distinct spectral lines in figure 1 by thermal diffusion.

2. Binary and ternary patterns of nanocolloids deposition

We first demonstrate the selection of these discrete trajectories corresponding to the three dominant modes with a pair of symmetrically situated ground electrodes shown in figure 2(a). The conventional spray experimental setup [7] was used to generate the Taylor cone. A high

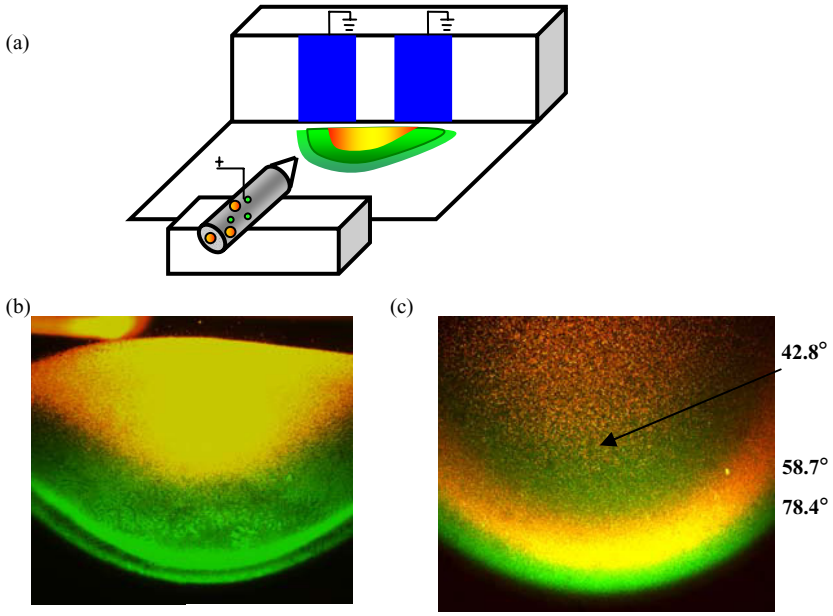

Figure 2. (a) The experimental setup with symmetrically placed ground electrodes with binary and ternary nanocolloid suspensions with diameters of 250, 400 and 980 nm. (b) The binary pattern with the zeroth mode selected by the 980 nm nanocolloid and deposition of different ring patterns by the 250 nm nanocolloid. (c) The ternary pattern with the zeroth mode selected by the 980 nm nanocolloid and deposition of different ring patterns by the 400 and 250 nm nanocolloids.

dc voltage was generated by A HCZE-30PNO25-LD high-voltage power supply (Matsusada Precision Device, Tokyo). A steel microneedle (Hamilton, 91033) with nominal outer diameter 210 μm and thickness 50 μm was filled with the working fluid and mounted on a glass stage 1 mm in height. The counter electrode pair are two paralleled strips of copper tape with a gap of 2.5 mm, placed about 2.0 mm away from the needle tip. Sufficient separation between the Taylor cone and the ground electrode and the height of the glass stage were allowed to ensure complete evaporation of liquid from the nanocolloids in flight. Liquid leaves distinctive stain marks on the substrate that disappear when the separation distance is beyond 2 mm and the height of the glass stage is beyond 1 mm for the applied voltage of about 2.0 kV used in this experiment. Since the working voltage window is bound between 1.8 and 2.5 kV due to cone formation and corona discharge, we cannot place the counter electrodes much further than the reported distance to further separate the nanocolloid deposition from the liquid stains. Individual nanocolloid deposition can be observed when imaged with an inverted fluorescent microscope (Olympus IX-71). The ring deposition was recorded by a high-performance quantitative digital CCD camera (QImaging Retiga-EXL). The working liquid is ethanol solution with 0.033% fluorescent nanoparticles. The nanocolloid suspension is either a binary mixture of 50% Fluoresbrite® Polychromatic Red Microsphere (Polyscience Inc.) with diameter of 980 nm and 50% green fluorescent microspheres (Duke Scientific Corp.) with diameter of 250 nm or an equal ternary mixture of the above two nanocolloids and a red-fluorescent 400 nm nanocolloid (Duke Scientific Corp.). The liquid conductivity was tuned by the addition of sodium chloride

and is measured to be 150 μs cm^{-1}. (See our earlier reference [9] on addition of salt to organic solvents.)

Figure 2(b) shows deposits of the binary nanocolloid suspension on the substrate between the Taylor cone and ground electrodes. Different fluorescent excitation differentiates the different nanocolloid deposits. The red 980 nm particles deposit into a full circle further from the cone with a polar angle of about 45°—they have selected the zeroth mode ($n = 0.5$) and the bunch of field extrema with polar angles less than 42.8° as shown in figure 1. The green 250 nm particles do indeed select ring harmonics by depositing in half rings closer to the cone. The first smaller half ring is deposited simultaneously with the full circle, followed by the next larger half ring. When the nanocolloids are sprayed individually, they select several modes—the zeroth mode in the center with a circular deposition pattern and several external bands corresponding to other modes. That two nanocolloids of different sizes in a binary suspension select different modes suggests that colloid interaction and separation must occur before the off-axis maxima are selected.

We note that the different deposition distance of the two nanocolloids, with the larger colloid traveling further, is just the opposite of what one would expect for a parabolic free fall due to gravity, whose force is about six orders of magnitude lower than the electrophoretic force. A similar separation of droplets of different sizes was observed in [10]. It is not known whether the size separation occurs at the tip of the cone before ejection or soon after ejection. It is expected, however, that each nanocolloid is surrounded only by neighbors identical to it at some point during the ejection. Unlike in solution, the Coulombic repulsion between the colloids is not screened in the gas phase. It is about 0.1 nN for a nanocolloid with an expected charge q of about 1.0×10^{-16} C. This repulsive force remains negligible compared to the tangential electrophoretic force on the nanocolloid, which is about 1.0 nN. However, the nanocolloid–nanocolloid repulsion force now dominates any electrophoretic force in the direction normal to the axis. The same Coulombic repulsion also suggests that nanocolloids that are closest to the axis and occupy the zeroth mode would repel other nanocolloids from the same field maximum. The actual transverse displacement from the axis is determined by the time of flight and higher charged particles with higher axial electrophoretic force and velocity are expected to be displaced less. The observed deposition patterns would then suggest that the larger particles hold more charge on their surface than the smaller ones and tend to populate the zeroth mode at the cone axis, whereas the smaller ones are repelled off axis to sample the discrete rings of the other modes. The charged solution on any particle is believed to lose liquid by charge-retaining evaporation and both charge and liquid by Rayleigh fission due to Coulombic repulsion [11]. For a liquid drop, this liquid/charge loss continues until the radius reaches the Rayleigh radius R governed by $q_R = 8\pi(\varepsilon_0 \gamma R^3)^{1/2}$ [12]. Liquid and charge loss from the nanocolloids by evaporation and Rayleigh fission is expected to proceed until this equilibrium drop radius is identical to the particle radius, lest the liquid does not evaporate completely or the particles acquire no charge from the solution—both unlikely propositions. As such, the total charge q_R on a particle increases with the particle size, as is consistent with the deposition patterns.

To confirm this mechanism, we show in figure 2(c) the deposition patterns of a ternary suspension, which produces a rainbow-like pattern with increasing particle sizes of 250, 400 and 980 nm away from the cone and with the smaller two nanocolloids selecting ring patterns. The smallest 250 nm green particles are mostly deposited into the outer band closest to the cone but some of them are also deposited into the inner bands dominated by the 400 and 980 nm

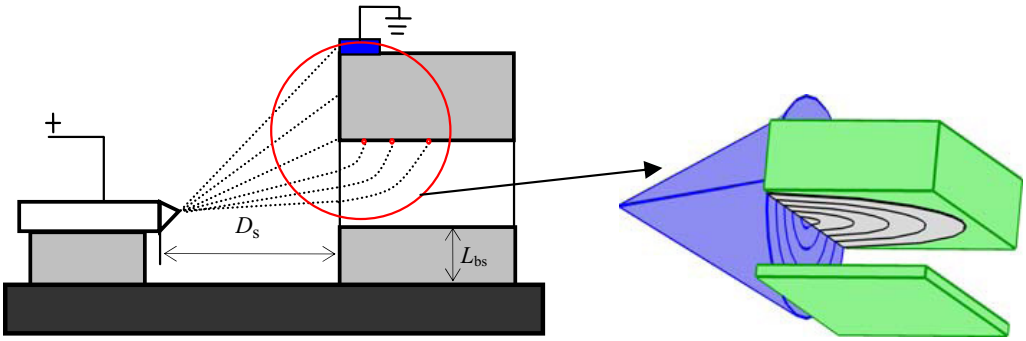

Figure 3. The experimental setup and a schematic of how the trajectories along the field maxima of the discrete harmonics in figure 1 intersect the slit entrance, with corresponding nanocolloid ring images on the substrate.

particles. We suspect this larger bandwidth is due to bead diffusion, as the electrophoretic force begins to diminish at this small size and the Péclet number approaches unity. Nevertheless, transverse displacement is sufficient to separate nanocolloids of different sizes such that they select different ring patterns. When we estimate the polar contact angles of each deposition ring by the vertical and lateral distances from the mid point of each ring to the cone, we obtain values of 76.3°, 60.9° and 41.2°, very close to the theoretical values of 78.4°, 58.7° and 42.8° in figure 1, corresponding to all the field maxima of the most dominant modes 2 and 3 away from the axis, confirming that the discrete maxima of the dominant cone harmonics are indeed captured.

3. Nanocolloid deposition spectrum inside a slit

Because of the dominance of the zeroth mode in figure 2, we are unable to access sufficient numbers of the discrete modes in figure 1 to obtain universal spectral lines. To completely screen the zeroth mode, we eject identical nanocolloids into a slit that is placed at an angle to the cone axis and attracted by a single asymmetric ground electrode, as shown in figure 3. One 1.2 mm slit was fabricated with two microscope slides (FisherBrand, 12-550-A3) and the slit was placed about 2.0 mm away from the needle tip. The thickness of the bottom slide is varied to position the slit at different vertical locations relative to the 1 mm high cone, thus allowing the capture of different harmonics. The bottom slide thickness L_{bs} is 1.5, 1.25 and 1.0 mm for cases (I)–(III) in figure 4, respectively. The counter electrode consisted of a strip of copper tape placed 1.5 mm above the slit. The working liquid is ethanol solution with 0.033% of the 980 nm red nanocolloid.

The Taylor cone axis is controlled by the ground position with one edge of the slit entrance closer to the cone than the other, such that only trajectories with a polar angle between about 20° and 55° relative to the cone axis can enter the slit. The initial deposition occurs at the outer edge of the slit. The deposited nanocolloids screen the field line connected to the edge and prevent further deposition there, forcing the ejected nanocolloids to sample the Taylor cone harmonics of figure 1 whose off-axis field maxima have polar angles within the allowed range—their field lines penetrate into the slit. The deposited nanocolloids at the outer edge hence act like the symmetric ground electrode pairs of figure 2 to excite the ring harmonics. Due to confinement

effects, the electric field within the slit is not dominated by the cone harmonics. The penetrated nanocolloids hence transfer from the cone field lines to the slit field lines and, due to inertia, deposit on the far substrate. A ring deposit is expected, corresponding to the image of the seventh harmonic on the substrate, as seen in figure 3. Once this ring is populated by the deposited nanocolloids, their screening effect compels the nanocolloids to sample the next discrete mode to affect sequential writing of colloid lines onto the top substrate of the slit.

This sequential writing of the ring deposits was indeed observed inside the slit for the geometries indicated. In the case figure 4(a), the deposition of the nine rings in figure 1 took about 4 h, with the first five rings taking about 3 min each and the last ring taking over 30 min. During the writing of each line, the nanocolloids deposit randomly along the ring at roughly the same rate. The curvature of the ring increases with each subsequent ring until the ring diameter becomes smaller than the slit width. The furthest penetration of the ring deposits is 0.37 cm, beyond which the deposition rate becomes negligible.

The ring patterns can be explicitly related to the Taylor cone harmonics via the universal polar angle separations seen in figure 1. As seen in figure 3, the longitudinal separation between two trajectories, corresponding to two different modes, can be related to the downstream separation between the corresponding two ring deposits on the substrate by a stretching affine transformation. This amounts to a linearization of the nanocolloid trajectory dynamics, such that, for a given cone/slit separation and cone angle, the difference in harmonic polar angles (along the field maxima) between two trajectories is proportional to the distance between the corresponding deposited rings. Because the field maxima of the harmonics in figure 1 are located at length scale-invariant polar angles, the intersection of these rays with a sufficiently narrow slit should occur at positions whose spacing obeys the same universal arc-length separations shown in figure 1. Another linear map relates these intersections with the slit entrance to the actual deposited lines. As such, the deposited rings for arbitrary cone location and angle should collapse into universal spectral lines after a simple shift to locate the same harmonic and a stretching affine transformation to account for the cone locations and inclinations. This is indeed observed in figure 4 for three cone angles and separations. For each set of deposited colloid lines, we locate an initial line that corresponds to the smallest ring (the first mode 7 ring) of figure 1 and stretch all the remaining lines to see if the stretched lines coincide with the remaining theoretical lines. With a few missing lines, all three deposited line collections align with the theoretical ones of figure 1, which is shown as a top ruler. We also offer a more explicit collapse of all three sets of normalized data in figure 4(b).

4. Conclusion

We observed the selection of multiple discrete trajectories by nanocolloids ejected from a Taylor cone, corresponding to the discrete harmonics. The binary and ternary patterns were formed by the particles of different sizes due to different residue charge. A sequential writing of the deposit spectrum was observed inside the microslit because the screening effect of the deposit rings compels the nanocolloids to sample the discrete mode of the harmonics. Precise writing of universal nanocolloid lines onto a planar surface or microslit substrates, with different particles selecting different spectral lines, should have extensive applications in macro-molecule mass spectrometry, electrostatic aerosol filtration and differential colloid mobility analysis. As suggested by the larger bandwidth of the 250 nm green particles in figure 2(c), bead diffusion is expected to smear these lines below a particle radius of 200 nm. Particles larger than 1 μm

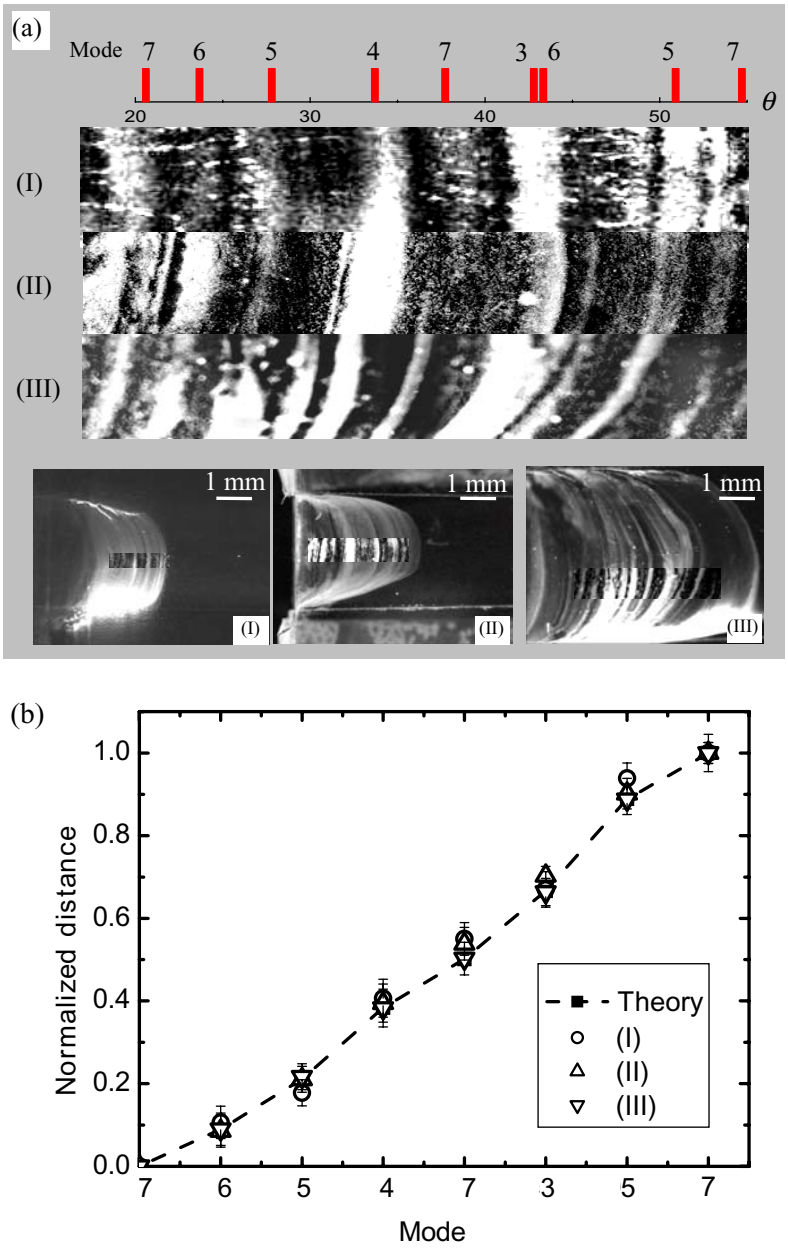

Figure 4. (a) The raw deposited rings with cone separation D_s and bottom slide thickness L_{bs} of about (2.0, 2.2, 2.2 mm) and (1.5, 1.25, 1.0 mm) are shown on the same scale in the three frames at the bottom. The boxes shown in the bottom three frames are stretched and shifted to produce the top three frames. The universal theoretical spectrum of figure 1 is also shown with the specific mode number and polar angle. (b) The collapsed curve of normalized ring positions measured from the slot entry. The distances of the first and last lines from the slot entry are normalized to the same position for all three sets of data.

would not be properly ejected out of the Taylor cone. As a consequence, we expect the lines can only be written with particles with diameters roughly between 100 nm and 1 μm. An intriguing new direction is to carry out ac electrospray of nanocolloids [9, 13], in addition to Coulombic repulsion, dielectrophoretic force, which is estimated to be 0.1 nN for 100 nm nanocolloids can be used to separate colloids of different surface conductance, conductivity and permittivity, as all have been shown to sensitively affect the dielectrophoretic mobility of nanocolloids [14].

Acknowledgments

We thank Nishant Chetwani for helpful discussions. This work was supported by the DTRA (HDTRA1-08-C-0016).

References

[1] Fenn J B, Mann M, Meng C K, Wong S F and Whitehouse C M 1989 *Science* **246** 64
[2] Loscetales G, Barrero A, Guerrero I, Cortijo R, Marquez M and Ganan-Calvo A M 2002 *Science* **295** 1695
[3] Salata O V 2005 *Curr. Nanosci.* **1** 25
[4] Taylor G I 1964 *Proc. R. Soc.* A **280** 383
[5] Rayleigh L 1945 *The Theory of Sound* (New York: Dover)
[6] Flagan R C 2001 *Electrical Techniques in Aerosol Measurement* (New York: Wiley)
[7] Wang P, Maheshwari S and Chang H-C 2006 *Phys. Rev. Lett.* **96** 254502
[8] Boltachev G Sh, Zubarev N M and Zubareva O V 2008 *Phys. Rev.* E **77** 056607
[9] Chetwani N, Maheshwari S and Chang H-C 2008 *Phys. Rev. Lett.* **101** 204501
[10] Tang K and Gomez A 1994 *Phys. Fluids* **6** 2317
[11] Lebarle P and Tang L 1993 *Anal. Chem.* **65** 972A
[12] Rayleigh L 1882 *Phil. Mag.* **14** 184
[13] Yeo L, Lastochkin D, Wang S-C and Chang H-C 2004 *Phys. Rev. Lett.* **92** 133902
[14] Basuray S and Chang H-C 2007 *Phys. Rev.* E **75** 060501